THE JOURNAL OF PHYSICAL CHEMISTRY C

Article

pubs.acs.org/JPCC

Evidence from 900 MHz ^{1}H MAS NMR of Displacive Behavior of the Model Order–Disorder Antiferroelectric $NH_4H_2AsO_4$

Jin Jung Kweon,[†] Riqiang Fu,*[,†] Jason A. Kitchen,[†] Peter L. Gor'kov,[†] William W. Brey,[†] and Naresh S. Dalal*[,†,‡]

[†]National High Magnetic Field Laboratory, Florida State University, 1800 E. Paul Dirac Drive, Tallahassee, Florida 32310, United States

[‡]Department of Chemistry and Biochemistry, Florida State University, Tallahassee, Florida 32306, United States

Supporting Information

ABSTRACT: $NH_4H_2AsO_4$ (ADA) is a model compound for understanding the mechanism of phase transitions in the KH_2PO_4 (KDP) family of ferroelectrics. ADA exhibits a paraelectric (PE) to antiferroelectric (AFE) phase transition at $T_N \sim 216$ K whose mechanism remains unclear. With the view of probing the role of the various protons in the transition mechanism, we have employed the high-resolution technique of magic angle spinning at the high Zeeman field of 21.1 T (^{1}H resonance at 900 MHz). We measured the temperature dependence of the isotropic chemical shift and spin–lattice relaxation time, T_1, of the O–H···O and NH_4^+ protons through the T_N. As $T \rightarrow T_N$, NMR peaks from the PE and AFE phases are seen to coexist over a temperature range of about 3 K, showing formation of nearly static (lifetime > milliseconds) pretransitional clusters in this lattice as it approaches its T_N, consistent with the near first-order nature of the phase transition. The isotropic chemical shift of the O–H···O protons exhibited a steplike anomaly at T_N, providing direct evidence of displacive character in this lattice commonly thought of as an order–disorder type. No such anomaly was noticeable for the NH_4^+ protons. Both sets of protons exhibited order–disorder characteristics in their T_1 data, as analyzed in terms of the standard Bloembergen, Purcell, and Pound (BPP) model. These data suggest that the traditionally employed classification of equilibrium phase transitions into *order–disorder* and *displacive* ones, should rather be "*order–disorder cum displacive*" type.

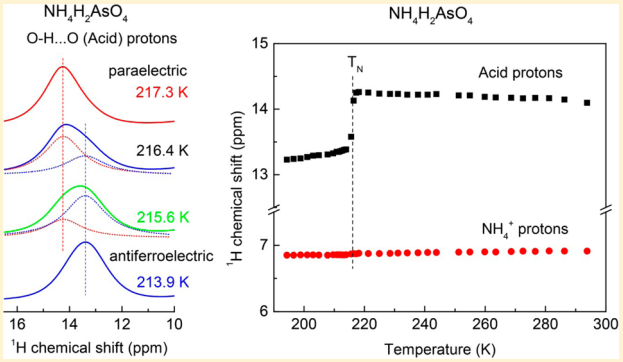

1. INTRODUCTION

The mechanism of ferroelectricity in the KH_2PO_4 (KDP) type hydrogen-bonded compounds has been studied extensively over the past several decades because of their applications in a wide range of technology such as laser frequency multiplication and related electro-optic applications as well as for understanding the roles of hydrogen-bonded protons in causing phase transitions.[1,2] This role is evident most directly from the fact that upon H → D substitution (i.e., deuteration) their ferroelectric (FE) transition temperature (T_c) or the antiferroelectric (AFE) transition temperature (T_N) increases drastically, an example being KDP itself where the T_c increases from 123 to 224 K.[1,2] While considerable progress has been made in understanding the FE phenomenon, much less is understood regarding the atomistic details of the AFE behavior.[1,2] A case in point is that only recently has it been theoretically proposed how the substitution in KDP of K^+ by NH_4^+ renders antiferroelectricity to this (FE) lattice: a cooperative interaction between the NH_4^+ group and the O–H···O (acid) protons due to the slowing down of the NH_4^+ ion's hindered rotation as $T \rightarrow T_N$ forces an AFE order in the H_2PO_4 units.[3,4] But a long-standing unanswered question is whether the phase transition is caused by mainly the order–disorder motion of the O–H···O protons in their double-minimum potential well coupled with the hindered-rotational hopping of the NH_4^+ groups, with the arsenate framework being essentially a buffer holding the H's in a double-minimum well (an order–disorder transition[1,2]), or whether the transition involves electronic structure changes in the whole molecular framework (as in a traditionally defined displacive transition[1,2]). Earlier attempts to answer this question for several hydrogen-bonded compounds have utilized NMR spectroscopy, since the time scale of the anticipated proton-lattice motion falls in the NMR regime (millisecond to picosecond).[4−6] These studies include (i) ^{31}P NMR on KD_2PO_4,[7] (ii) ^{13}C on squaric acid,[8,9] (iii) ^{15}N for $NH_4H_2AsO_4$ (ammonium dihydrogen arsenate, ADA)[10,11] and ammonia borane[12] and ^{1}H for ADA[13,14] and $NH_4H_2PO_4$ (ammonium dihydrogen phosphate, ADP),[15,16] but the experimental methods used in the earlier studies were different from that of the present work. The ^{15}N study on ADA[10,11] used the NH_4^+

Received: December 5, 2014
Revised: February 9, 2015
Published: February 20, 2015

DOI: 10.1021/jp512127x
J. Phys. Chem. C 2015, 119, 5013−5019

cation as a probe of displacive character at the cation site and did not search for the order−disorder aspect. Studies utilizing ^{1}H as a probe[13−16] used such a low resolution that the peaks from the NH_4^+ and O−H···O protons were strongly overlapped; it was thus not possible to ascertain their specific roles. A closely relevant result is the earlier conclusion from ^{31}P chemical shift studies on KD_2PO_4 that its ferroelectric transition is purely of the order−disorder type,[7] based on the observation (within large error bars) that the ^{31}P isotropic chemical shift, δ_{iso}, was found to be essentially temperature independent around T_c. It has, however, been later shown to be inaccurate[17] because on repeating the experiment with enhanced spectral resolution, reducing the signal line width via magic angle spinning (MAS), the ^{31}P δ_{iso} in KD_2PO_4 was seen to change anomalously on going through T_c.[17] Another shortcoming of the earlier NMR studies was the use of rather low (<1 T) Zeeman fields[7,8] because the studies involved mainly relaxation as a probe, which for these cases seemed to be more sensitive to molecular dynamics at low Zeeman fields.[7−16] The present study was thus undertaken to circumvent these deficiencies. Here, we have increased the resolution by orders of magnitude by working at the highest available uniform Zeeman field of 21.1 T (i.e., 900 MHz resonance frequency for ^{1}H)[18] and utilizing the MAS technique employing single crystals.[19−21] We selected ADA because its T_N of 216 K is well within the variable temperature range available with the 900 MHz spectrometer at the National High Magnetic Field Laboratory in Tallahassee, FL.[18] The experiments involved the measurement of the temperature dependence of δ_{iso}, as well as spin−lattice relaxation times (T_1), of the O−H···O and NH_4^+ protons individually, since these two parameters provide complementary information on the nature of the phase transition.[4−17] δ_{iso} is known to be quite sensitive to electronic structure change in the whole molecular orbital framework around a given atom, but not to simple reorientational or translational changes.[4−6] An observed anomalous change in δ_{iso} at a phase transition is therefore considered to be a direct evidence of a displacive character of the transition. For an order−disorder transition, δ_{iso} should remain essentially unchanged, or it changes smoothly on cooling through a phase transition. Temperature variation of T_1, on the other hand, would shed direct light on the motional dynamics of the ligands around the probed nucleus and hence probe the order−disorder character of the phase transition. Our data reported herein strongly suggest that the AFE transition in ADA contains characteristics of both an order−disorder and a displacive transition. This is considered a somewhat novel concept in the thermodynamic classification of equilibrium phase transitions, since traditionally equilibrium phase transitions are classified as either order−disorder or displacive kind. We envisage that the current ultrahigh-resolution ^{1}H NMR study of the ADA phase transition should find wider applications.

2. EXPERIMENTAL DETAILS

Single crystals of ADA were grown by room temperature evaporation of an aqueous reaction mixture of $(NH_4)_2CO_3$ with As_2O_5 (both from Alfa Inorganics).[10,11] A small piece of visually defect-free crystal (~1 × 1 × 1 mm^3) was packed in a 3.2 mm MAS rotor and used for MAS NMR measurements in order to obtain higher resolution by obviating the anisotropic bulk magnetic susceptibility.[19−21] The ^{1}H MAS NMR line-shape and T_1 measurements were performed on a ultrawide bore (UWB) 900 MHz magnet equipped with a Bruker Avance III NMR console.[18] A standard $\pi/2-\tau-\pi-\tau$ spin−echo pulse sequence, where 2τ is the echo time, was used to record ^{1}H signals in order to suppress the ^{1}H background signals from the probe components. Adamantane (1.63 ppm, relative to TMS) was used as the chemical shift reference.[22] The inversion recovery method combined with the spin−echo sequence, i.e., $\pi-$recovery$-\pi/2-\tau-\pi-\tau$, was used for the T_1 measurements. The ^{1}H MAS NMR spectra and T_1 measurements were recorded using a recycle delay of 5 s and a spinning speed of 13.5 kHz. Although a higher spinning is possible with our current equipment and better in terms of narrowing the ^{1}H resonances, we chose 13.5 kHz in our experiments to ensure that the crystal sample used remained intact during the sample spinning. Under the sample spinning condition, the spin echo was always set to be synchronized with the rotor echoes; i.e., the delay τ plus the π pulse length was equal to a multiple of the spinning period. It is worth noting that combining spin-space averaging with MAS is popular for ^{1}H line-narrowing in solids.[23] However, an effective spin-space decoupling requires *long and strong* ^{1}H radio-frequency (rf) irradiation, which could introduce additional but transient rf heating on the sample, especially at higher fields (i.e., higher frequencies).[24] In order to avoid the temperature uncertainty due to the rf heating on the ADA sample involving the paraelectric (PE)−antiferroelectric (AFE) phase transition within a few degree of temperature, we chose the simple MAS method.

The variable-temperature (VT) ^{1}H NMR experiments were performed using an XR902A12 AirJet sample cooler (SP Scientific) for cooling the bearing channel (to a minimum of 203 K) and a modified Doty Scientific liquid nitrogen heat exchanger for cooling the VT channel. Sample temperatures were regulated through the VT channel using a Bruker BVT-3000 unit with the accuracy of ±0.1 K. The temperature range of measurement was from 294 to 194 K. The NMR spectra were collected at 0.8 K intervals around T_N ± 5 K, and 2−5 K intervals at other temperatures, with a waiting time of at least 5 min for temperature equilibrium at each point. The sample temperature was calibrated in separate experiments using ^{207}Pb NMR of diluted lead nitrate (mixed with KBr at a mass ratio of 1:1). The value of T_N was defined as the temperature where the relative intensities of coexisting two phases are the 1:1 ratio.

An NHMFL-designed and fabricated 3.2 mm HX double resonance MAS probe (shown in Figure 1) was used for low-

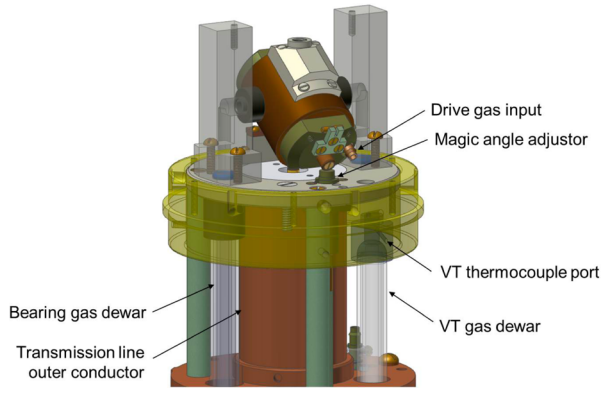

Figure 1. View of 900 transmission line 3.2 mm MAS probe head, showing VT, bearing, and magic angle adjustment components.

DOI: 10.1021/jp512127x
J. Phys. Chem. C 2015, 119, 5013−5019

temperature VT experiments on the 900 UWB magnet. The design was based upon the transmission line circuit of an earlier developed static probe,[18] with added features to allow for low-temperature VT experiments to 130 K. The circuit utilizes a ^{1}H-X double tuned single solenoid rather than a cross coil. Both channels are electrically balanced, the ^{1}H channel through a sleeve balun and the X channel through a removable chip capacitor. The X channel is broadband through removable chip capacitors which can be added in parallel to the tuning variable capacitor. The stator (Varian, Inc., modified with help from Revolution NMR, Ft. Collins, CO) uses a 3.2 mm pencil style rotor to minimize the sample thermal gradient by locating the drive turbine cap farther from the sample space than in other 3.2 mm rotor designs. There are also baffle plates between the sample space and bearings in order to minimize convective thermal mixing of the sample and room temperature drive gas. VT and bearing gas are both delivered to the stator through vacuum insulated glass dewars, and the stator was modified to route each gas through the stator posts in order to minimize thermal losses. Users are able to connect the XR902A12 Airjet sample cooler directly to the bearing input port at the probe base, and the bearing channel input temperature can be precisely controlled from 190 to 370 K. Cooling the bearing gas not only lowers the sample temperature by approximately 50 K but also allows for further sample thermal gradient reduction by matching the VT and bearing gas temperatures. The temperature calibration using the $Pb(NO_3)_2$ sample packed in the center of a 3.2 mm rotor with a thickness of ~5 mm is shown in the Supporting Information. When the VT and bearing gas temperature matched, the temperature gradient was as small as ~1 K across the sample volume (~5 mm thickness in the center of a 3.2 mm rotor). When they mismatched, the temperature gradient was as large as 12 K. Therefore, by minimizing the temperature difference between the VT and bearing gas, we can greatly minimize the temperature gradient across the sample volume, a crucial factor for studying materials involving coexisting phases in a rather small temperature range. In earlier ^{15}N studies we broke the sample in 1/2, twice, and found that the coexistence range did not change the observed coexistence range appreciably.[9−12]

In addition, the modification also involved in the magic angle (MA) setting device. MA is adjusted via a micrometer-type differential screw mechanism, which provides an effective 1.5 mdeg fine change in magic angle per degree of mechanism rotation. The MA adjustor is located directly behind the stator housing; the short length of the contact between the screw mechanism and stator body serves to minimize thermal contraction and expansion effects that might lead to angle instability during wide VT experiments. The 50 L heat exchanger cryostat used to cool VT channel nitrogen gas is refilled automatically from a 180 L liquid nitrogen supply cryostat, allowing for extended duration experiments, such as overnight operation.

3. RESULTS AND DISCUSSION

A. Crystal Structure. Figure 2 shows the three-dimensional crystal structure of ADA in the PE phase,[1,2] where the AsO_4 and NH_4^+ groups locate alternatingly along the *c*-axis. In this phase (above ~216 K), ADA exhibits tetragonal symmetry, space group $I\bar{4}2d$, with the tetragonal axis of the AsO_4 groups coinciding with the crystal *c*-axis. The AsO_4 groups are linked by hydrogen bonds in a three-dimensional way. In the popular model of the phase transition, the protons play the crucial role.

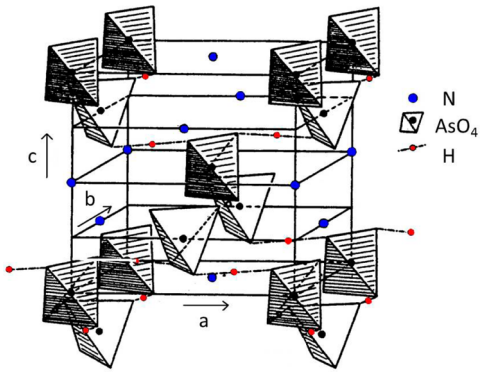

Figure 2. Schematic representation of $NH_4H_2AsO_4$ (ADA) in the PE phase, after ref 1.

At $T > T_N$, the O−H···O protons are delocalized between the two minima positions of a double-minimum potential well along the O−H···O bond. At $T < T_N$, they are localized at one or the other position of this double minimum potential well, thus lowering the symmetry to $P2_12_12_1$ in the AFE phase.[25,26] However, X-ray crystal structure studies could not distinguish between a *dynamic versus static* disorder. To answer this query, NMR studies were undertaken by several authors.[7−16] Because of their major aim on measuring molecular dynamics, the studies were focused mainly on the spin−lattice relaxation phenomenon which is more effective at low Zeeman fields. At these low fields, however, the spectral resolution was insufficient to disperse the chemical shifts of NH_4^+ peaks from those of the O−H···O protons. These issues provided us strong impetus for undertaking the current study at a much higher Zeeman field.

B. ^{1}H NMR at 900 MHz: Spectra and Peak Assignment. Figure 3 shows the comparison between ^{1}H signals from an

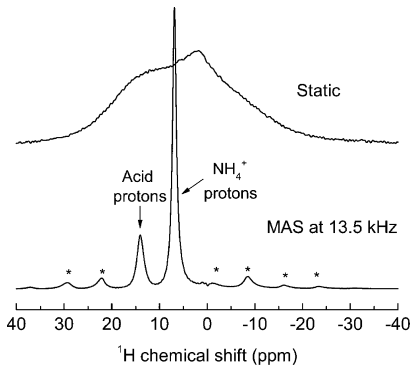

Figure 3. ^{1}H static (top) and MAS (bottom) spectra at 900 MHz of an ADA single crystal at room temperature with the echo time of 140 μs. The asterisks mark the spinning sidebands.

ADA crystal at static (top) and MAS (bottom) conditions. ADA has two types of (the acid and ammonium) protons and each of them gives rise to a different anisotropic resonance depending on the crystal orientation in the magnetic field. In addition, the presence of strong proton homonuclear dipolar couplings significantly broaden their resonances so that the acid and ammonium protons are severely overlapped and cannot be distinguishable, as indicated in Figure 3 (top). On the other hand, fast MAS not only removes the anisotropic chemical shifts, resulting in their orientational independent isotropic resonances, but also partially suppresses the proton homo-

DOI: 10.1021/jp512127x
J. Phys. Chem. C 2015, 119, 5013−5019

nuclear dipolar couplings. Consequently, the ^{1}H resolution under fast MAS is greatly enhanced as shown in Figure 3 (bottom), and the acid and ammonium protons can now be resolved.

Figure 4 shows a room-temperature ^{1}H MAS NMR spectrum of ADA at 900 MHz using a spinning speed of 13.5 kHz. The

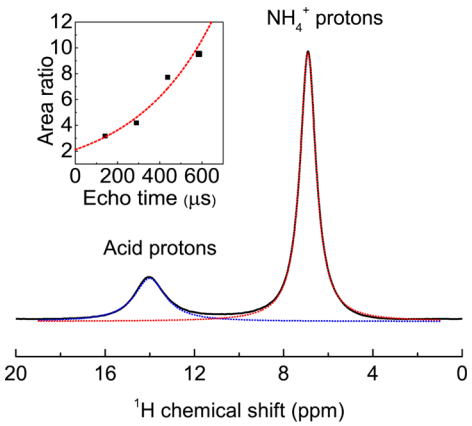

Figure 4. ^{1}H MAS spectrum of an ADA single crystal at 900 MHz recorded at room temperature with the echo time of 140 μs. Inset shows that the area ratio of the NH_4^+ to acid protons as a function of the echo time approaches 2:1 with decreasing echo time.

two well-resolved peaks can easily be assigned: the two H's of the O−H···O (acid) units and the four H's of NH_4^+ groups, as marked. Apparently, the line width of the acid protons is larger than that of the NH_4^+ protons, owing to motional narrowing due to a much faster C4 hindered rotation associated with the NH_4^+ groups. Consequently, due to their shorter spin−spin relaxation time (T_2), the FID of the acid protons decays faster than that of the NH_4^+ protons, so that the observed ratio of the peaks from the NH_4^+ and acid protons in Figure 3 was 3.2, i.e., a lot more than the expected value of 2. The inset of Figure 4 shows that the area of peaks for the NH_4^+ and acid protons approaches the expected 2:1 ratio with decreasing echo time in the spin−echo sequence.

As mentioned earlier, a major goal of this study was to measure the temperature dependence of the isotropic chemical shifts, δ_{iso}, of the two sets of protons on going through the T_N, i.e., to determine whether δ_{iso} remains essentially unchanged (sign of an order−disorder transition) or whether it changes anomalously (as for a displacive transition).[4−12] Figure 5 shows the temperature dependence of the δ_{iso} upon cooling through T_N. Clearly the δ_{iso} of the acid protons undergoes a significant abrupt change around the transition temperature T_N, implying the presence of a *displacive* character for the acid protons while taking part in the AFE phase transition. For the NH_4^+ protons, on the other hand, the δ_{iso} remains essentially unchanged through the T_N, showing that the NH_4^+ groups execute essentially an order−disorder dynamics, albeit at a slower rate, as shown in section D (*vide infra*).

C. Coexistence of Paraelectric and Antiferroelectric Phases. Figure 6 shows the temperature dependence of the line widths of the acid and NH_4^+ protons. The line widths of the NH_4^+ protons have much smaller values than those of the acid protons due to the fast rotational motion of the NH_4^+ protons. The change of line width of the NH_4^+ protons is minimal over the entire temperature range measured. On the other hand, the line width for the acid protons exhibits a sharp

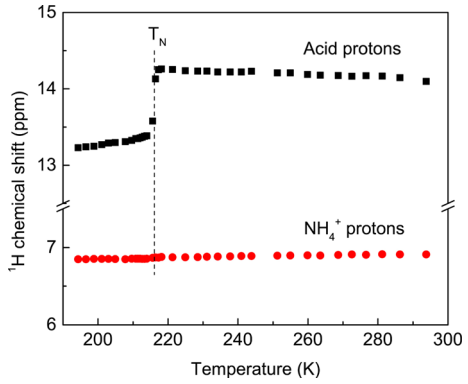

Figure 5. Temperature dependence of ^{1}H chemical shift of the acid and NH_4^+ protons of ADA at 900 MHz using 13.5 kHz spinning speed.

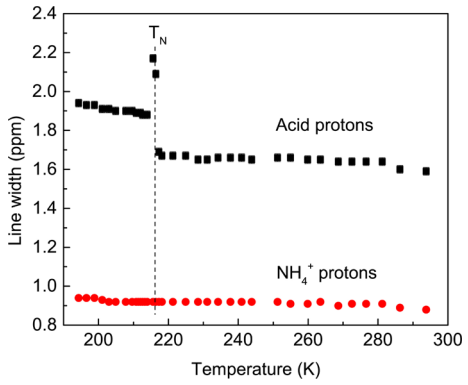

Figure 6. Temperature dependence of ^{1}H line widths of the acid protons and NH_4^+ protons.

increase as $T \rightarrow T_N$, while shows little variation at $T > T_N$. This significant increase in line width of the acid protons was observed in the vicinity of T_N, an clear evidence of the order−disorder characteristic.

Figure 7a shows ^{1}H MAS NMR spectra of the O−H···O protons in the close vicinity of the phase transition temperature

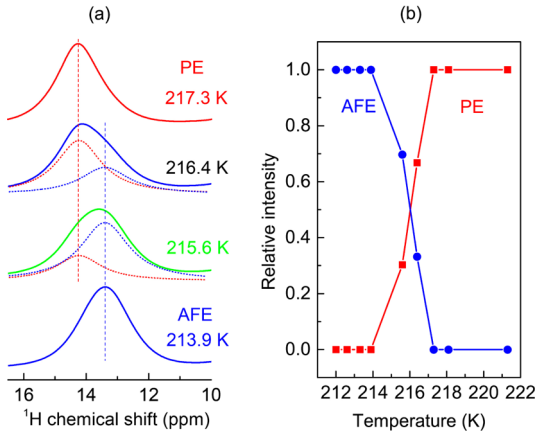

Figure 7. (a) Temperature dependence of the 900 MHz ^{1}H MAS peaks of the acid protons in ADA around T_N. The coexistence of the peaks from the PE and AFE portions of the crystal lattice is clearly seen within about 3 K of T_N. (b) Relative intensities of the two phases in the vicinity of T_N. Detailed testing showed that the gradient across the crystal was no more than 1 K.

DOI: 10.1021/jp512127x
J. Phys. Chem. C 2015, 119, 5013−5019

T_N = 216 K. The line shapes at 215.6 and 216.4 K could not be fitted with a single resonance as at 213.9 and 217.3 K, while their line widths at half-height are significantly larger than those at 213.9 and 217.3 K. In order to deconvolute the peaks at 215.6 and 216.4 K, we first fitted the line shapes at 213.9 and 217.3 K and then used their respective line widths and positions as constants to deconvolute the line shapes at 215.6 and 216.4 K by varying their relative intensities. Clearly, the deconvoluted spectra fit quite well, showing that the signals were indeed a result of an overlap of those from the PE and AFE phases. Figure 7b shows the deconvoluted intensities of the acid protons around T_N. The relative intensities show that the peak from the PE phase at δ_{iso}^{PE} = 14.2 ppm and that from the AFE phase at δ_{iso}^{AFE} = 13.4 ppm coexist within 3 K around T_N. We emphasize that the large discontinuity in the isotropic chemical shift across the phase transition (from δ_{iso}^{PE} = 14.2 ppm to δ_{iso}^{AFE} = 13.4 ppm) is an accepted, clear evidence of the displacive character of the phase transition.[4−6] On the other hand, the NH_4^+ protons showed relatively little discontinuity, in accordance with the earlier conclusion that the NH_4^+ protons execute essentially an order−disorder dynamics at the (subnanosecond) NMR time scale. This conclusion is not in contradiction to the X-ray structural report that the NH_4^+ units lose their tetrahedral symmetry at $T < T_N$, in view of the much faster (femtosecond) time scale of the X-ray measurements.[1,2,4−6]

D. ^{1}H Spin−Lattice Relaxation, T_1. The VT ^{1}H T_1 measurements were made to further understand the motional dynamics of both sets of protons at the Larmor frequency of 900 MHz. The spin−lattice relaxation rates $(1/T_1)$ of the O−H···O (acid) and the NH_4^+ protons follow a similar pattern, as can be seen from Figure 8. These data demonstrate that the

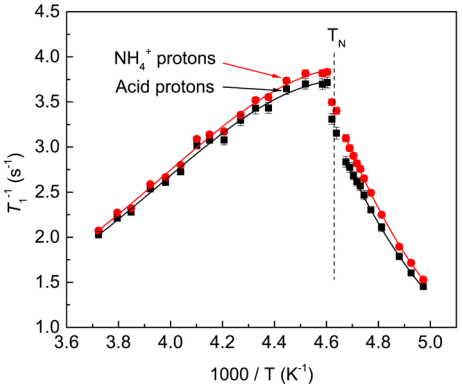

Figure 8. Temperature dependence of T_1 rates (T_1^{-1}) of both protons in ADA at 900 MHz, using 13.5 kHz spinning speed.

acid and NH_4^+ protons reach a common spin temperature and relax at a common rate.[27] It is evident from Figure 8 that there exists a discontinuity at around T_N, implying that an anomalous change does take place in the proton dynamics around T_N. The ^{1}H NMR spin−lattice relaxation rates (T_1^{-1}) below and above T_N were fitted to the Bloembergen−Purcell−Pound (BPP) model:[28−30]

$$T_1^{-1} = \frac{2}{3}\gamma^2 M_2 \left[\frac{\tau_c}{1 + (\omega_0\tau_c)^2} + \frac{4\tau_c}{1 + (2\omega_0\tau_c)^2} \right] \quad (1)$$

$$\tau_c = \tau_0 \exp[E_a/RT] \quad (2)$$

where γ is the proton gyromagnetic ratio, M_2 the second moment, ω_0 the Larmor frequency, E_a the activation energy, R the gas constant, and τ_0 the infinite-temperature correlation time. The M_2, E_a, and τ_0 were considered as variables in the fittings.

The activation energies (E_a) and pre-exponential factors (τ_0) of the acid protons obtained from the fittings are 5.0 ± 0.2 kcal/mol and (4.1 ± 3.2) × 10^{-15} s (below T_N) and 2.7 ± 0.1 kcal/mol and (2.0 ± 0.5) × 10^{-13} s (above T_N), respectively. Those of the NH_4^+ protons were 5.1 ± 0.2 kcal/mol and (3.7 ± 2.8) × 10^{-15} s (below T_N) but 2.6 ± 0.1 kcal/mol and (2.2 ± 0.5) × 10^{-13} s (above T_N), respectively. For both sets of protons, the activation energies at the AFE and PE phases are similar to those reported in the earlier static ^{1}H NMR studies.[13,14]

Using the E_a and τ_0 values, we calculated the correlation times (τ_c) of the acid and NH_4^+ protons. Figure 9 shows that

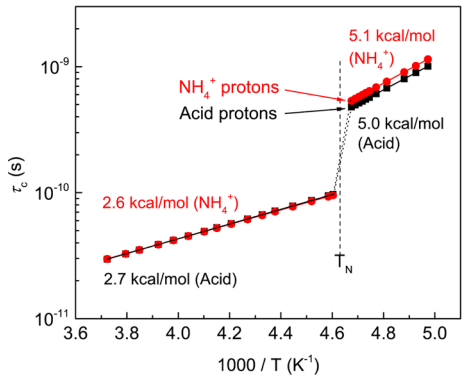

Figure 9. Temperature dependence of τ_c of protons in ADA across T_N.

the τ_c's of both sets are nearly the same, and both change significantly below T_N. As in eq 2, the slopes of ln τ_c vs 1000/T below and above T_N represent the activation energies of the acid and NH_4^+ protons, as derived by fitting of T_1 rates.

An important observation was that the averages of the activation energies and τ_0's in the PE as well as the AFE phases *for both sets of protons* are comparable to those of N atom as obtained from ^{15}N T_1 data.[11] This result implies that both sets of protons experience the same relaxation mechanism, and they reach the same equilibrium spin temperature in both the PE and AFE phases. Based on the BPP theory, the dipole−dipole interaction constant, as defined by

$$C = \frac{2}{3}\gamma^2 M_2 = \frac{3}{10}\left(\frac{\mu_0}{4\pi}\frac{\gamma^2\hbar}{r_{HH}^3}\right)^2 \quad (3)$$

is used to characterize the dipolar−dipolar distances responsible for the dominant relaxation mechanism. From the crystal structure at 220 K of paraelectric phase,[25,26] the distance between the ammonium and acid protons, $r_{HH} = d(H_N\cdots H_O) \sim$ 2.028 Å, while the proton distance within the NH_4^+ group is ~1.527 Å. Our BPP model fittings resulted in the M_2 value for the acid protons of (49.7 ± 11.0) × $10^{-8}T^2$ (below T_N) and (31.2 ± 0.40) × $10^{-8}T^2$ (above T_N), respectively, and for the NH_4^+ protons of (60.2 ± 15.0) × $10^{-8}T^2$ (below T_N) and (32.4 ± 0.5) × $10^{-8}T^2$ (above T_N), respectively. Thus, the proton distances yielded for the dominant dipolar relaxation mechanism in eq 3 were 1.38 ± 0.30 Å (below T_N) and 1.50 ± 0.02 Å (above T_N) for the acid protons and 1.34 ± 0.50 Å

DOI: 10.1021/jp512127x
J. Phys. Chem. C 2015, 119, 5013−5019

(below T_N) and 1.49 ± 0.02 Å (above T_N) for the NH_4^+ protons. Clearly, in the PE phase (above T_N), the obtained dipolar−dipolar distances responsible for the relaxation in both the acid and ammonium protons are quite consistent with that derived from the crystal structure within the NH_4^+ group.[25,26] While in the AFE phase (below T_N) the calculated dipolar−dipolar distances for both the acid and ammonium protons are significantly shorter than the proton−proton distance within the NH_4^+ protons, an evidence for the slowing down of the NH_4^+ reorientational motion in the AFE phase. Therefore, the relaxation mechanism is indeed dominated by the fast reorientational motion and dipolar fluctuations due to this motion.[7−16] Interestingly, the activation energies increase by a factor of nearly 2, while the correlation time τ_c increases by 1 order of magnitude from the PE to the AFE phase, implying that the motion of both types of protons slows down on entering the AFE phase.

Clearly, the T_1 measurements primarily characterize the motion of the NH_4^+ groups in ADA. Slowing down of the reorientational motion of the NH_4^+ groups at T_N evidently suggests that one of the four protons in the NH_4^+ groups starts to form an N−H···O bond, thus leading to a localization of the O−H···O protons in one of the two minima of their O−H···O bond, supporting directly the theoretical model of antiferroelectric transition in ADP (and by implication, ADA) by Lasave et al.[3] It seems worth clarifying that the goal of the present work was quite distinct from that of Lasave et al.[3] and in fact all other earlier studies:[6−16] This study looked for evidence for displacive behavior of this model order−disorder lattice, whereas Lasave et al.[3] examined primarily the role of hydrogen bonding between the NH_4^+ ion and the O's of the PO_4^{3-} ion as the basis of the antiferroelectric character in ADP (and by extension for ADA) as compared to the ferroelectric nature of KH_2PO_4. Other differences are discussed in the Introduction.

4. CONCLUSIONS

This study shows that utilization of high-field (900 MHz) MAS ^{1}H NMR measurements offers advantages not possible with much lower Zeeman fields. It enables us to probe the mechanism of the PE−AFE phase transition in ADA to an unprecedented detail, using the acid (O−H···O) and NH_4^+ protons as probes for the first time in this class of materials. A microscopic snapshot of the phase transition is evident from the rarely reported phenomenon of coexistence of NMR peaks from two phases of a material as its lattice feels the onsetting of an ensuing phase transition. An important part of the study was to ensure that the coexistence of the peaks representing the PE and AFE phases was not an artifact of 2−3 K range of temperature gradient across the used small (∼1 mm^3) crystal. This was based on detailed temperature calibration using $Pb(NO_3)_2$, different sample sizes, and cold gas flow rates. The results clearly and strongly suggest that on approaching T_N, from the high temperature side, within 2−3 K, the lattice first breaks down into small regions that exhibit the symmetry of the low temperature while the temperature is high enough that sample is still mainly in the high-temperature phase. Earlier NMR attempts to detect such pretransitional clusters in ADA (using ^{75}As Zeeman perturbed NQR) did not succeed, likely due to the much broader signals (lower resolution).[31] Notable also is that the acid protons clearly exhibit "displacive" features on approaching the T_N, since their δ_{iso} changed abruptly on passing through the phase transition. The chemical shift of the NH_4^+ protons, on the other hand, exhibited little anomaly, implying that the NH_4^+ groups execute their motional dynamics the same as at higher temperatures albeit at a slower rate. The relaxation data of both sets of protons is quite consistent with an "order−disorder" behavior. The ADA phase transition thus exhibits, *simultaneously*, features of both "order−disorder" and "displacive" type. These results suggest that the traditional classification of equilibrium phase transitions into "order−disorder" and "displacive" types is not general enough; there should also be another category, "order−disorder *cum* displacive" phase transitions. We envisage that the present study will elicit renewed interest in the high-field, high-resolution NMR studies of phase transitions in polar solids.

■ ASSOCIATED CONTENT

Supporting Information

Temperature calibration using the $Pb(NO_3)_2$ sample packed in the center of a 3.2 mm rotor with a thickness of ∼5 mm showing temperature gradient across the sample volume; complete ref 18. This material is available free of charge via the Internet at http://pubs.acs.org.

■ AUTHOR INFORMATION

Corresponding Authors

*(N.D.) Tel 850-644-3398; Fax 850-644-8281; e-mail dalal@chem.fsu.edu.

*(R.F.) Tel 850-644-5044; Fax 850-644-1366; e-mail rfu@magnet.fsu.edu.

Notes

The authors declare no competing financial interest.

■ ACKNOWLEDGMENTS

We are grateful for financial support from the User Collaboration Grants Program (UCGP) at the National High Magnetic Field Laboratory (NHMFL) which is supported by National Science Foundation (NSF) Cooperative Agreement DMR-1157490, the State of Florida, and the U.S. Department of Energy. We thank Dr. Ilya Litvak for design of the differential pitch magic angle mechanism and Prof. Hans Jakobsen, Drs. Ivan Hung, and Zhehong Gan for help identifying thermally induced changes in the stator angle on the previous design iteration.

■ REFERENCES

(1) Lines, M. E.; Glass, A. M. *Principles and Applications of Ferroelectrics and Related Materials*; Oxford University Press: New York, 2001.

(2) Blinc, R.; Zeks, B. *Soft Modes in Ferroelectrics and Antiferroelectrics*; North-Holland: Amsterdam, 1974.

(3) Lasave, J.; Koval, S.; Dalal, N. S.; Migoni, R. L. Origin of Antiferroelectricity in $NH_4H_2PO_4$ from First Principles. *Phys. Rev. Lett.* **2007**, *98*, 267601.

(4) Blinc, R. Ferroelectrics 1966−2001: An Overview. *Ferroelectrics* **2002**, *267*, 3−22.

(5) Blinc, R. Order and Disorder in Perovskites and Relaxor Ferroelectrics. *Struct. Bonding (Berlin)* **2007**, *124*, 51−67.

(6) Bussmann-Holder, A.; Dalal, N. S. Order-Disorder versus Displacive Dynamics in Ferroelectric Systems. *Struct. Bonding (Berlin)* **2007**, *124*, 1−21.

(7) Blinc, R.; Burgar, M.; Rutar, V.; Seliger, J.; Zupančič, I. ^{31}P Chemical-Shift Study of the Ferroelectric Transition in KD_2PO_4. *Phys. Rev. Lett.* **1977**, *38*, 92−95.

(8) Mehring, M.; Becker, J. D. Observation of Electronic Structure Change at the First-Order Phase Transition in Quasi-Two-Dimen-

DOI: 10.1021/jp512127x
J. Phys. Chem. C 2015, 119, 5013−5019

sional Squaric Acid ($H_2C_4O_4$) by ^{13}C NMR. *Phys. Rev. Lett.* **1981**, *47*, 366−370.
(9) Dalal, N.; Klymachyov, A.; Bussmann-Holder, A. Coexistence of Order-Disorder and Displacive Features at the Phase Transitions in Hydrogen-Bonded Solids: Squaric Acid and its Analogs. *Phys. Rev. Lett.* **1998**, *81*, 5924−5927.
(10) Dalal, N. S.; Gunaydin-Sen, O.; Fu, R.; Achey, R.; Pierce, K. L. High Resolution NMR Evidence for Displacive Behavior in Hydrogen-Bonded Ferroelectrics and Antiferroelectrics. *Ferroelectrics* **2006**, *337*, 3−12.
(11) Gunaydin-Sen, O.; Fu, R.; Achey, R.; Dalal, N. S. Order-Disorder and Displacive Behavior of the Cation (NH_4^+) Sites in the Hydrogen-Bonded Antiferroelectric $NH_4H_2AsO_4$: ^{15}N NMR Evidence. *Ferroelectrics* **2006**, *337*, 153−160.
(12) Gunaydin-Sen, O.; Achey, R.; Dalal, N. S.; Stowe, A.; Autrey, T. High Resolution ^{15}N NMR of the 225 K Phase Transition of Ammonia Borane (NH_3BH_3): Mixed Order-Disorder and Displacive Behavior. *J. Phys. Chem. B* **2007**, *111*, 677−681.
(13) Grosescu, R. NMR Study of Molecular Reorientations in $NH_4H_2AsO_4$. *Chem. Phys. Lett.* **1973**, *21*, 80−82.
(14) Dalal, N. S.; McDowell, C. A.; Srinivasan, R. Magnetic Resonance Studies of the Antiferroelectric Phase Transitions in the Ammonium Arsenates $NH_4H_2AsO_4$ and $ND_4D_2AsO_4$. *J. Chem. Phys.* **1974**, *60*, 3787−3794.
(15) Kasturi, S. R.; Moran, P. R. Study of Antiferroelectric Ammonium Dihydrogen Phosphate (ADP) by Pulsed NMR. *Phys. Rev. B* **1975**, *12*, 1874−1884.
(16) Ripmeester, J. A.; Dalal, N. S. Anomalous ^1H Spin-Lattice Relaxation in Antiferroelectric Ammonium Dihydrogen Phosphate (ADP). *Phys. Rev. B* **1978**, *18*, 3739−3741.
(17) Bussmann-Holder, A.; Dalal, N. S.; Fu, R.; Migoni, R. High-Precision ^{31}P Chemical Shift Measurements on KH_2PO_4-Type Crystals: Role of Electronic Instability in the Ferroelectric Transition Mechanism. *J. Phys.: Condens. Matter* **2001**, *13*, L231−237.
(18) Fu, R.; Brey, W. W.; Shetty, K.; Gor'kov, P.; Saha, S.; Long, J. R.; Grant, S. C.; Chekmenev, E. Y.; Hu, J.; Gan, Z.; et al. Ultra-Wide Bore 900 MHz High-Resolution NMR at the National High Magnetic Field Laboratory. *J. Magn. Reson.* **2005**, *177*, 1−8.
(19) Vanderhart, D. L.; Earl, W. L.; Garroway, A. N. Resolution in ^{13}C NMR of Organic Solids Using High-Power Proton Decoupling and Magic-Angle Sample Spinning. *J. Magn. Reson.* **1981**, *44*, 361−401.
(20) Fu, R.; Gunaydin-Sen, O.; Dalal, N. S. Simultaneous Supralinear Line-Narrowing and Sensitivity Enhancement at High Fields in Magic Angle Spinning NMR of Spin-1/2 Nuclei in Solids. *J. Am. Chem. Soc.* **2007**, *129*, 470−471.
(21) Dugar, S.; Fu, R.; Dalal, N. S. Increasing ^{13}C CP-MAS NMR Resolution Using Single Crystals: Application to Model Octaethyl Porphyrins. *J. Phys. Chem. B* **2012**, *116*, 9215−9222.
(22) Harris, R. K.; Becker, E. D.; Cabal De Menezes, S. M.; Granger, P.; Hoffman, R. E.; Zilm, K. W. Further Conventions for NMR Shielding and Chemical Shifts IUPAC Recommendations 2008. *Solid State Nucl. Magn. Reson.* **2008**, *33*, 41−56.
(23) Ryan, L. M.; Taylor, R. E.; Paff, A. J.; Gerstein, B. C. An Experimental Study of Resolution of Proton Chemical Shifts in Solids: Combined Multiple Pulse NMR and Magic-Angle Spinning. *J. Chem. Phys.* **1980**, *72*, 508−515.
(24) Li, C.; Mo, Y.; Hu, J.; Chekmenev, E.; Tian, C.; Gao, F. P.; Fu, R.; Gor'kov, P.; Brey, W.; Cross, T. A. Analysis of RF Heating and Sample Stability in Aligned Static Solid-State NMR Spectroscopy. *J. Magn. Reson.* **2006**, *180*, 51−57.
(25) Fukami, T. X-Ray Study of Crystal Structure of $NH_4H_2AsO_4$ in the Paraelectric and Antiferroelectric Phases. *Phys. Status Solidi A* **1990**, *121*, 383−390.
(26) Fukami, T. Refinement of the Crystal Structure of $NH_4H_2AsO_4$ Above and Below Antiferroelectric Phase-Transition Temperature. *J. Phys. Soc. Jpn.* **1989**, *58*, 3429−3430.
(27) Bloembergen, N.; Shapiro, S.; Pershan, P. S.; Artman, J. O. Cross-Relaxation in Spin Systems. *Phys. Rev.* **1959**, *114*, 445−459.
(28) Bloembergen, N.; Purcell, E. M.; Pound, R. V. Relaxation Effects in Nuclear Magnetic Resonance Absorption. *Phys. Rev.* **1948**, *73*, 679−712.
(29) Slichter, C. P. *Principles of Magnetic Resonance*; Springer: Berlin, 1990.
(30) Abragam, A. *Principles of Nuclear Magnetism*; Oxford University Press: Oxford, 1983.
(31) Adriaenssens, G. J. On the ^{75}As NMR Spectrum in Paraelectric $NH_4H_2AsO_4$. *Ferroelectrics* **1976**, *12*, 269−271.

DOI: 10.1021/jp512127x
J. Phys. Chem. C 2015, 119, 5013−5019